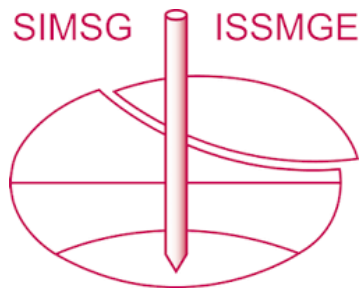


INTERNATIONAL SOCIETY FOR SOIL MECHANICS AND GEOTECHNICAL ENGINEERING



This paper was downloaded from the Online Library of the International Society for Soil Mechanics and Geotechnical Engineering (ISSMGE). The library is available here:

<https://www.issmge.org/publications/online-library>

This is an open-access database that archives thousands of papers published under the Auspices of the ISSMGE and maintained by the Innovation and Development Committee of ISSMGE.

The paper was published in the Proceedings of the 8th International Symposium on Deformation Characteristics of Geomaterials (IS-PORTO 2023) and was edited by António Viana da Fonseca and Cristiana Ferreira. The symposium was held from the 3rd to the 6th of September 2023 in Porto, Portugal.

Apparatus for swelling deformation of compacted bentonite utilizing multi-ring moulds for evaluation of dry density and water content distribution

Daichi Ito^{1#}, Hailong Wang¹, and Hideo Komine¹

¹Waseda University, 3-4-1, Okubo, Shinjuku, Tokyo, Japan

[#]Corresponding author: daichi_ito@aoni.waseda.jp

ABSTRACT

In the geological disposal of high-level radioactive waste, bentonite buffer materials are required to have self-sealing property, which is the ability to fill gaps by swelling deformation between the buffer material and the waste containment vessel or surrounding bedrock. Self-sealing property was evaluated based on the pressure generated after the gap filling under the assumption of constant dry density and water content in the specimen and buffer material. On the other hand, it takes tens to hundreds of years for the transitional period until the buffer contacts with groundwater, fills the gap, and the internal state converges to a uniform state. To assess changes more accurately in the condition of the buffer material, it is necessary to evaluate time courses in the density and water content of the buffer material because of groundwater infiltration and swelling deformation. From these, the authors developed an experimental apparatus for swelling deformation of bentonite, which consists of a mould with 2 mm-thick stacked rings. It is aimed to evaluate the distribution of dry density, water content, and degree of saturation inside the specimen by cutting the specimen with a 2 mm thick ring after the end of experiment. In this paper, results of preliminary experiments to confirm the applicability of this apparatus to swelling deformation test of bentonite was firstly described. Then, experiments were conducted on compacted bentonite specimens using this apparatus, and changes in the dry density and water content distribution inside the specimens were evaluated in terms of swelling deformation behaviour.

Keywords: Bentonite; Swelling deformation; Multi-ring mould; Geological disposal.

1. Introduction

For the geological disposal of high-level radioactive waste, bentonite materials are planned to be compacted and used as a buffer material around the waste (Pusch, 1992; Sellin and Leupin, 2013.). Bentonite buffer material is required to meet multiple performance requirements, including low permeability and self-sealing capability, etc. The self-sealing capability indicates the ability of filling gaps between the waste container, bedrock, and buffer material by swelling deformation (Numo, 2021.). If these gaps are not well filled, it may become leakage paths for radionuclides, therefore, self-sealing capability is an important performance in conducting a safety assessment of the repository. Gap filling by swelling deformation associated with water absorption is a coupled behavior of

soil deformation and water movement. Although several studies have attempted to model this phenomenon (Smiles and Rosenthal, 1968; Philip, 1969.), it has not yet been established well.

In most of the previous studies, the self-sealing property was evaluated based on the pressure generated after the gap was filled, assuming that the dry density and water content of the specimen and buffer material were uniform (Komine et al. 2004; Wang, et al. 2013; Jia et al. 2019; Bian et al. 2019; Watanabe and Yokoyama, 2021.). On the other hand, transition period of several tens to several hundreds of years is required from the moment for the buffer material contacts with groundwater, and then fills the gap, and the distribution of dry density and water content may converge to a uniform state as shown in Fig. 1. Few study have examined the internal dry density distribution associated with self-sealing of buffer material in laboratory and full-

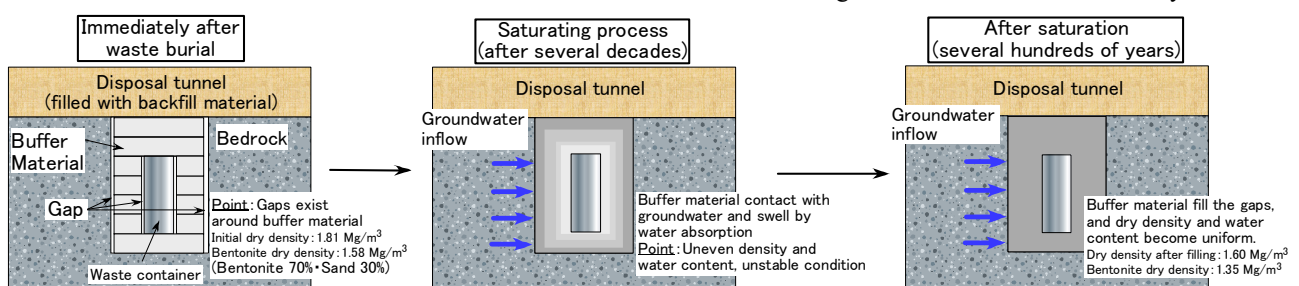


Figure 1. Change in condition of buffer material because of groundwater inflow.

scale experiments (SKB, 2019.), but the data and conditions were limited and have not yet been theoretically verified. To improve the accuracy of monitoring for buffer material condition, it is necessary to understand the state changes associated with swelling deformation behavior during the gap filling process from both experimental and theoretical perspectives.

In this study, swelling deformation test, which simulates low-constraint conditions during gap filling, were conducted on compacted bentonite specimens under constant loading (20 kPa) using a device with multi-ring moulds to experimentally evaluate changes over time in the internal distribution of dry density, water content, and degree of saturation.

2. Material and test device

2.1. Bentonite used in this study

A Japanese commercial bentonite powder (Kunigel-V1, K_V1) was used for this study. It has been used in many previous studies relating the Japanese geological disposal project. The basic characteristics of K_V1 are shown in Table 1. Montmorillonite content was obtained by methylene blue adsorption test, and is 52.8%. Leached cations were processed and measured with benzyltrimethylammonium chloride, and dominant cation is Na^+ . Particle size of K_V1 were adjusted less than $50 \mu\text{m}$ (Wang et al. 2020). The sample was stored in the airtight container, and initial water content of the sample was in the range of 8.9~9.3%.

Table 1. Basic characteristics of K_V1.

Soil particle density (Mg/m^3)	2.76
Liquid limit (%)	535.4
Plastic limit (%)	26.7
Plasticity index	508.7
Content of montmorillonite (%)	52.8
Leached Na^+ ion (cmol/kg)	53.8
Leached Ca^{2+} ion (cmol/kg)	35.5
Leached Mg^{2+} ion (cmol/kg)	4.1
Leached K^+ ion (cmol/kg)	1.6

2.2. Test system of swelling deformation with multi-ring moulds

Swelling deformation tests were conducted using the system presented in Fig. 2. The system consisted of a test cell, a displacement gauge, a water inlet burette, and a vertical load. In the test cell, the specimen was confined radially by a mould, and the vertical swelling deformation was measured under a constant loading pressure (20 kPa). The test cell consisted of a bottom plate, a mould, a top plate, and a piston. The bottom plate had three holes, from which water was supplied to the specimen. The mould consisted of a set of 2 mm thick stainless rings with an inner diameter of 28 mm, and between two 2 mm rings, a 0.30 mm thick two-sheet ring was set as shown in Fig. 3. Note that the inside wall of the 2 mm rings was not chamfered to reduce undetectable deformation in the lateral direction and leakage of the specimen between the rings. A fixing vessel was provided outside the ring laminate to prevent the mould

from moving during the experiment. A displacement gauge with a minimum scale of 0.002 mm and a capacity of 25 mm was used for swelling deformation measurement. Membrane filters, with a pore size of $0.45 \mu\text{m}$ and a thickness of $140 \mu\text{m}$, were placed at the top and bottom surfaces of the specimen. The hydraulic gradient at the beginning of the test was approximately 130, and it decreased as the water level in the burette decreased due to water absorption and swelling deformation of the specimen.

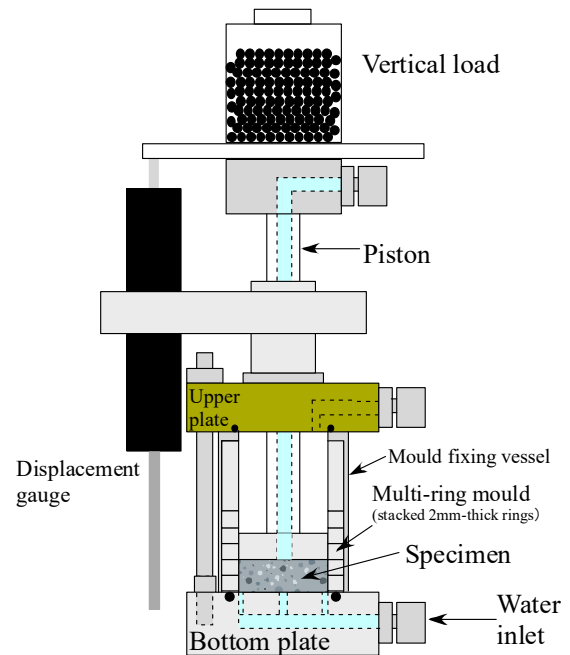


Figure 2. Swelling deformation apparatus with multi-ring mould.

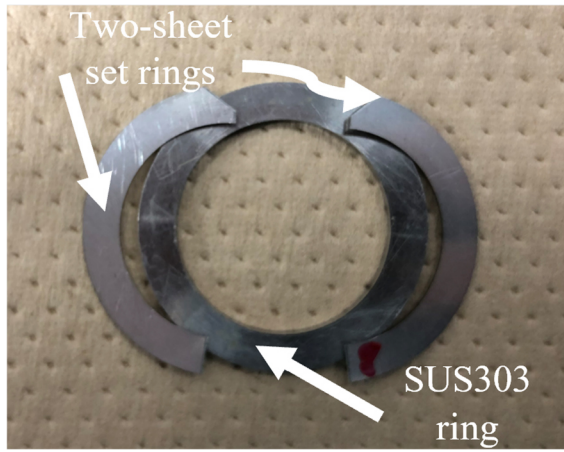


Figure 3. Appearance of stainless ring and two-sheet ring.

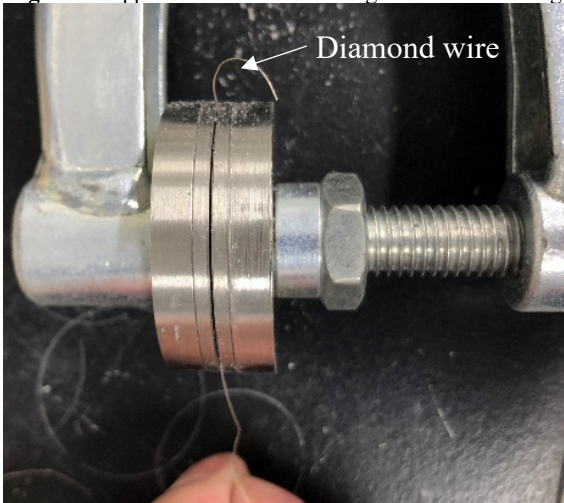


Figure 4. View of cutting specimen with diamond-wire.

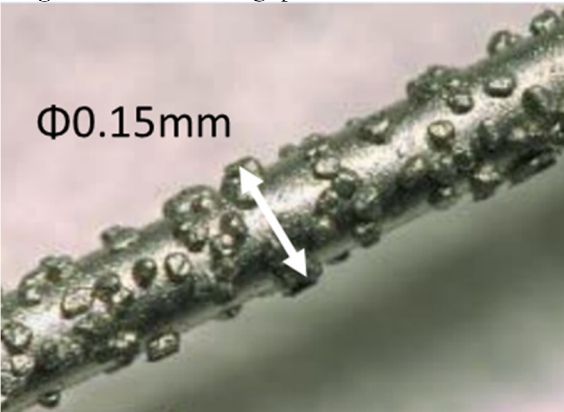


Figure 5. Enlarged view of diamond wire (additions to Ei Research website).

Five specimens with a diameter of 28 mm and a thickness of 4.3 mm, as shown in Table 2, were prepared.

Table 2. Swelling deformation test cases.

Initial dry density (Mg/m ³)	Test period (day)	Mould type
1.61	8	Normal
1.59	8	
1.34	1	Multi-ring
1.33	3	
1.32	7	
1.33	11	

The purpose of these cases was to confirm the repeatability of the swelling deformation behavior and to obtain changes over time in the dry density, water content, and degree of saturation distribution. Also, another specimen which had same diameter and thickness was also tested with a 50 mm height mould to investigate the friction effect. To prepare the specimen, K_V1 powder was directly compacted into the mould which consisted of 2 stainless rings and a two-sheet rings. Compaction was performed in one direction using a piston, and the side of the piston was set as the underside of the specimen. The specimen weight was measured up to 1 μ g, and height was measured to the nearest 1 μ m.

After the test cell was assembled, a loading weight was placed on the top plate. Water was supplied from the bottom of the specimen, and deformation measurement were simultaneously started. After the test periods shown in Table 2 had elapsed, the test cell was dismantled. During disassembly of the mould, the two-sheet ring was firstly removed, and the specimen was sliced every 2 mm using diamond wire whose diameter was 0.15 mm, as shown in Fig. 4 and Fig. 5. The use of ring laminates and the method of specimen division were conducted in accordance with Wang et al. (2020) and Ito and Komine (2022). After shaping the specimens with faces aligned with the ring surface, the mass of the specimen and water content was measured. Based on these data, the dry density and degree of saturation of each section were calculated. The swelling deformation measured with a displacement gauge was divided by the initial height of the specimen using Eq. (1) to obtain the swelling strain.

$$\varepsilon_s = \frac{\Delta S}{H_0} \times 100 \quad (1)$$

In this equation, ε_s : swelling strain, ΔS : Swelling deformation; and H_0 : Initial specimen height (=4.3 mm).

3. Results and discussion

3.1. Effect of side wall effect using multi-ring moulds

To understand the side wall friction effect of the multi-ring mold on swelling deformation behavior, the time history of the swelling strain was compared between the multi-ring mould and the 50 mm height mould (normal mould) compacted at a dry density of around 1.6 Mg/m³. Fig. 6 shows the time history of swelling strain comparing the multi-ring and normal mould. From this, in both cases, the increase in swelling strain was almost identical during the entire test period, indicating that the influence of the multi-ring mould was small. In addition, when the mould was split after the experiment, no leakage of specimens or water was observed between the molds. Therefore, the mould was applicable to experiments on swelling deformation of bentonite.

3.2. Repeatability of time history of swelling deformation curve

In Fig. 7, time course of swelling strain are shown for four specimens with initial dry densities ranging from

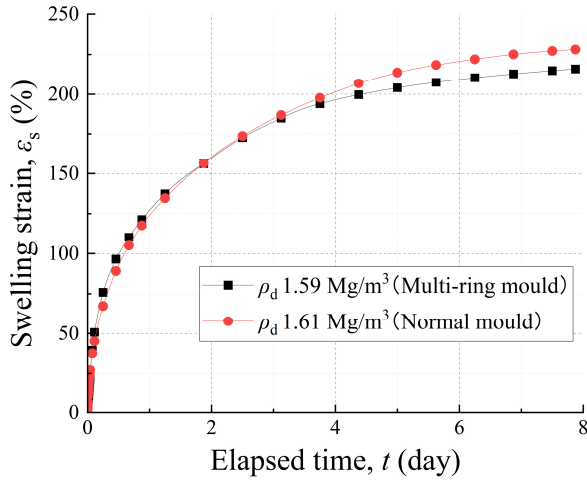


Figure 6. Time course of swelling strain comparing with multi-ring and normal mould.

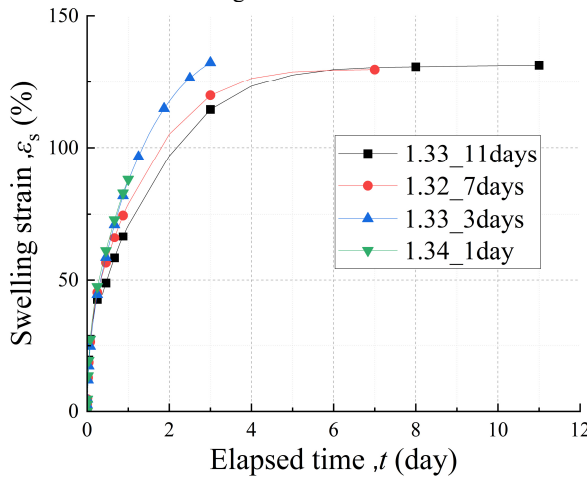


Figure 7. Time course of swelling strain with initial dry density of 1.32~1.34 Mg/m³.

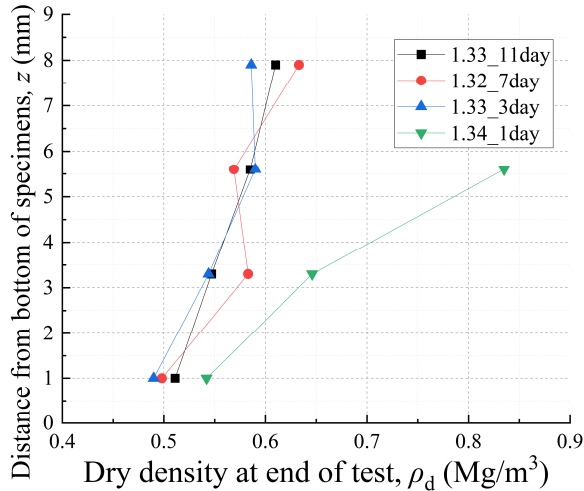


Figure 8. Relation between distance from bottom of specimen z and dry density.

1.32 to 1.34 Mg/m³ for experimental periods of 1, 3, 7, and 11 days. Although there were some differences in swelling strain value in the case of 3 days, these cases shows almost the same time course. Therefore, it indicates this test system has high repeatability.

3.3. Distribution of dry density, water content, and degree of saturation in the specimens

Fig. 8 shows the relation between the distance from bottom of specimen z and the dry density at the end of the test. The center of each mold height is used as the representative value for the distance from the water supply surface. The results show that the dry density tends to increase toward the top of the specimen for the 1 day test period, while for the 3 to 11 days test period, the dry density for all parts generally converges to 0.5 to 0.6 Mg/m³. Also in the case of 11 days, dry density of upper side was about 0.1 Mg/m³ lower than bottom of the specimen. There are two possible reasons for this: the density difference during compaction of the specimen may remain, or the dry density may not become uniform even after the swelling deformation are converged. To verify the first point, some specimens were prepared separately and were cut immediately after compaction, and the dry density of the compaction side and the opposite side were measured. The results are shown in Table 3.

Table 3. Results of dry density differences between compaction side and opposite side.

Target dry density (Mg/m ³)	1.3	1.6	1.9
Dry density of opposite side (Mg/m ³)	1.29	1.51	1.87
Dry density of compaction side (Bottom of swelling deformation test specimen) (Mg/m ³)	1.31	1.58	1.91

The dry density of the specimen with 1.3 Mg/m³ did not differ in the both side, suggesting that the density difference did not affect the results of this study. For the 1.6 Mg/m³ and 1.9 Mg/m³ specimens, the density was about 0.05 Mg/m³ higher on the compacted side, indicating that the initial density difference of the specimens should be considered when compacting to higher dry densities in the future studies. From these results, dry density may not become uniform, or quite long term may need for uniform density condition.

Fig. 9 shows the relation between z and the water content, and Fig. 10 shows the relation between z and the degree of saturation. Fig. 9 shows that the water content reached its maximum value at the bottom side, and tended to decrease as the distance from the water surface increased over test period. Fig. 10 shows that the degree of saturation distribution in all four cases tended to increase as the distance from the water supply surface increased, although there was some variation. In all cases, the degree of saturation was close to 90% or more. Fig. 9 shows the relation between z and the water content, and Fig. 10 shows the relation between z and the degree of saturation. Fig. 9 shows that the water content reached its maximum value at the bottom side, and tended to decrease as the distance from the water surface increased over test period.

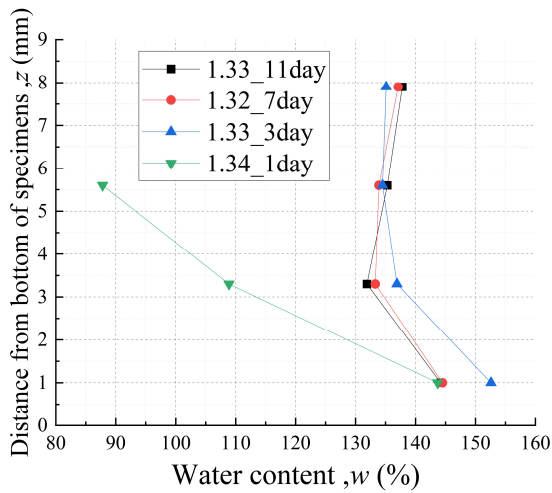


Figure 9. Relation between z and water content.

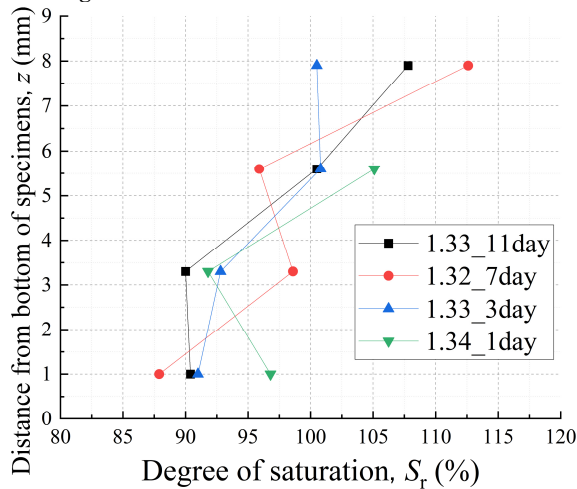


Figure 10. Relation between z and degree of saturation.

Fig. 10 shows that the degree of saturation distribution in all four cases tended to increase as the distance from the water supply surface increased, although there was some variation. In all cases, the degree of saturation was close to 90% or more. Also, in the case of one day, the dry density and water content deviated significantly from the other cases, while the degree of saturation was similar to the other cases. The possible reason for this is that the increase in water content and the decrease in dry density accompanying swelling deformation occur simultaneously, so that the denominator and numerator increase simultaneously in

terms of the definition equation for degree of saturation ($S_r = wG_s / (G_s / \rho_d - 1)$), and as a result, no large deviations in degree of saturation were observed. Shorter experiments would be necessary to evaluate the intra-specimen distribution of saturation.

One possible reason for degree of saturation exceeding 100% is that the porewater density of the bentonite may exceed 1 Mg/m^3 . In former experimental investigation, the porewater density was measured 1.05 to 1.08 Mg/m^3 in the dry density range of 0.5 to 0.8 Mg/m^3 (Wang, 2022.), which was the range of dry density at the end of test in this study. This is consistent with the results that the maximum measured saturation was about 110%.

In further study, tests will be conducted under a wider range of dry density and experimental period conditions, and aim to construct a theoretical model that can analyze water diffusion behavior and swelling and deformation behavior in unsaturated bentonite specimens.

4. Conclusions

The results of this paper are as follows.

- 1) The applicability of a multi-ring mould with stacked 2 mm thick rings to experiments on swelling deformation of bentonite was confirmed in this study, from the viewpoints of side wall friction effect on swelling deformation, no water and sample leakage between rings, and repeatability of time course of swelling strain.
- 2) The dry density, water content, and degree of saturation distribution were obtained for four cases of specimens with initial dry densities of 1.32 to 1.34 Mg/m^3 and experimental durations of 1, 3, 7, and 11 days.
- 3) The dry density difference about 0.1 Mg/m^3 were remained comparing upper and lower side of specimens while swelling strain were converged. On the other hand, when compacting specimen of 1.3 Mg/m^3 dry density, the difference in specimen was almost uniform. From the above, dry density may not become uniform, or quite long term may need for uniform density condition.

Acknowledgements

This study was supported through funding provided by the Kajima Foundation. This study was also supported

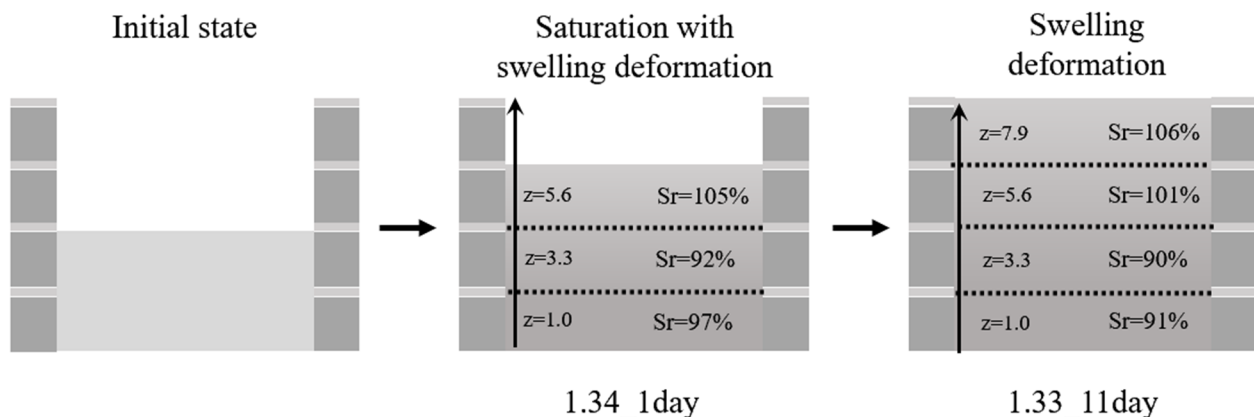


Figure 11. Schematic figure of time course of saturation and swelling deformation of specimen.

by the Ministry of Economy, Trade and Industry (METI) of Japan. Some of the present work was performed as a part of the activities of the Research Institute of Sustainable Future Society, Waseda Research Institute for Science and Engineering, Waseda University.

References

- Bian, X., Cui, Y.J., Li, X.Z. "Voids effect on the swelling behaviour of compacted bentonite", *Geotechnique*, Vol. 69, No. 7, pp. 593-605, 2019. <https://doi.org/10.1680/jgeot.17.P.283>
- Dueck, A., Börgesson, L., Kristensson, O., Malmberg, D., Akesson, M. and Hernelind, J.: "Bentonite homogenization -Laboratory study, model development and modelling of homogenisation processes", SVENSK KÄRNBRÄNSLEHANTERING AB, TR-19-11, p.78, 2019. <https://www.skb.com/publication/2494361>
- Ito, D. and Komine, H. "Experimental study to elucidate cementation effect on swelling pressure and montmorillonite basal spacing of bentonite ore", *Proceedings of 20th International Conference on Soil Mechanics and Geotechnical Engineering*, Vol.2, pp.3803-3808, 2022.
- Jia, L.Y., Chen, Y.G., Ye, W.M., Cui, Y.J. "Effects of a simulated gap on anisotropic swelling pressure of compacted GMZ bentonite", *Engineering Geology*, Vol. 248, pp. 155-163, 2019. <https://doi.org/10.1016/j.enggeo.2018.11.018>
- Komine, H., Ogata, N., Nakashima, A., Takao, H., Ueda, H., Kimoto, T. "Evaluation of self-sealing property of bentonite-based buffer by one-dimensional model test", *Journal of JSCE III*, Vol. 66, pp. 101-112, 2004. https://doi.org/10.2208/jscej.2004.757_101
- NUMO (Nuclear Waste Management Organization of Japan). "The NUMO Pre-siting SDM-Based Safety Case", NUMO-TR-21-01, p.4-40, 2021. https://www.numo.or.jp/technology/technical_report/pdf/NUMO-TR21-01_rev220222.pdf
- Philip, J. R. "Hydrostatics and hydrodynamics in swelling soils", *Water Resources Research*, Vol. 5, No. 5, pp. 1070-1077., 1969. <https://doi.org/10.1029/WR005i005p01070>
- Pusch, R. "Use of bentonite for isolation of radioactive waste products", *Clay Minerals*, Vol. 27, pp. 353-361, 1992. <https://doi.org/10.1180/claymin.1992.027.3.08>
- Sellin, P. and Leupin, O.X. "The use of clay as an engineered barrier in radioactive-waste management – A review", *Clays and Clay Minerals*, Vol. 61, No. 6, pp. 477-498, 2013. <https://doi.org/10.1346/CCMN.2013.0610601>
- Smiles, D. E. and Rosenthal, M. J. "The movement of water in swelling materials", *Australian Journal of Soil Research*, Vol. 6, No. 2, pp. 237-248, 1968. <https://doi.org/10.1071/SR9680237>
- Wang, H., Shirakawabe, T., Komine, H., Ito, D., Gotoh, T., Ichikawa, Y., Chen, Q. "Movement of water in compacted bentonite and its relation with swelling pressure", *Canadian Geotechnical Journal*, Vol. 57, pp.921-932, 2020. <https://doi.org/10.1139/cgj-2019-0219>
- Wang, H.: Pore water density in a saturated bentonite, *Géotechnique*, 2022. <https://doi.org/10.1680/jgeot.22.00247>.
- Wang, Q., Tang, A.M., Cui, Y.J., Delage, P., Barnichon, J.D., Ye, W.M. "The effect of technological voids on the hydro-mechanical behaviour of compacted bentonite-sand mixture", *Soils and Foundations*, Vol. 53, No. 2, pp. 232-245, 2013. <https://doi.org/10.1016/j.sandf.2013.02.004>
- Watanabe, Y. and Yokoyama, S. "Self-sealing behavior of compacted bentonite-sand mixtures containing technological voids", *Geomechanics for Energy and the Environment*, Vol. 25, 100213, 2021. <https://doi.org/10.1016/j.gete.2020.100213>